Ljungstrom, A. M.; Monro, Tanya Mary.
Exploration of self-writing and photosensitivity in ion-exchanged waveguides, *Journal of the Optical Society of America B - Optical Physics*, 2003; 20 (6):1317-1325.

Exploration of self-writing and photosensitivity in ion-exchanged waveguides

Ami M. Ljungström and Tanya M. Monro

Optoelectronics Research Centre, University of Southampton, Southampton SO17 1BJ, UK

Received November 27, 2002; revised manuscript received January 23, 2003

We have demonstrated that self-written channel waveguides can be formed reproducibly in K^+-ion-exchanged Nd-doped Bk7 glass by making use of a photosensitive index change of $\sim 6 \times 10^{-5}$ induced by illumination at 457 nm. The guidance characteristics of these waveguides have been investigated from 457 to 1550 nm. Detailed experiments have been carried out by exploration of the self-writing process, and these are also used to investigate the photosensitivity of the material. We find that an intensity threshold exists below which photosensitivity does not occur. Numerical simulations of both the evolution and the guidance properties of the self-written waveguides provide excellent agreement with observations.

OCIS codes: 130.2790, 190.5940, 230.7370, 230.7380.

1. INTRODUCTION

Self-written waveguides can evolve if a beam of light is focused onto and allowed to propagate through a photosensitive material.[1–3] A Gaussian beam focused onto a photosensitive sample initially diffracts, and since photosensitive index changes occur more rapidly where the intensity is high, the material undergoes the fastest changes at the input face and along the propagation axis. In many materials light causes the index to increase, which reduces the initial diffraction of the Gaussian writing beam. In the early stages an adiabatic taper forms, and over time a channel waveguide can be induced throughout the sample. These are called self-written waveguides (SWWs) as the same light that induces the waveguide is also guided by it.

These waveguides can offer a range of potential advantages over current waveguide fabrication methods such as epitaxial growth, diffusion methods, and direct writing.[2] For example, self-writing is a one-step process that requires no translation or chemical processing. In addition, the choice of input beam determines the final waveguide shape. When a Gaussian beam is used, tapers or channels can be self-written, however, a more complicated writing beam, for example, a multipeaked beam, could ultimately create Y junctions or couplers.[4] Recent research into self-writing in photopolymers and UV-curable resins has shown that Y junctions can form by use of multiple writing beams[5] and low-loss interconnections between fibers have also been self-written.[6,7]

Here we explore the self-writing process in planar ion-exchanged silicate glass. Previously self-written channels in planar glass have been created in ion-implanted $Bi_4Ge_3O_{12}$,[8] germanosilicate glass,[1] and As_2S_3 chalcogenide glass.[9,10] In bulk geometry experiments have been carried out in gallium lanthanum sulfide chalcogenide glass[3] and in Nd-doped Bk7 glass.[11] So far only tapers and channels have been written experimentally in glass, although further progress has been made in photopolymers, largely because photopolymers exhibit reproducible photosensitivity that occurs rapidly (seconds) and large index changes can be obtained ($\Delta n < 0.03$).[7] This work in polymers demonstrates that self-writing is a powerful technique for creating novel waveguides, and similar improvements in glass would facilitate the development of solid devices with the advantage of ready integration with conventional technologies.

2. MATERIAL

To be a suitable host for self-writing, a material needs to undergo a significant index change in response to light to overcome the diffraction of the writing beam and to create a waveguide through the glass. Here we explore the self-writing process in planar geometry, as this geometry has the potential for facile integration with existing planar devices and sources.

We chose to use K^+-ion-exchanged Nd-doped Bk7 because Bk7 is a commercially available material with good spatial homogeneity. Also, gratings have been written in planar K^+-ion-exchanged silica by use of 351-nm light to induce index changes of 10^{-5}.[12] Such direct-writing processes make use of the absorption of light near the band edge. However, in self-writing, the writing beam must propagate through the whole sample length. Hence light above the band edge can be used to induce a multiphoton absorption process (and thus change the refractive index) without inducing significant loss. We find that illumination of K^+-ion-exchanged undoped Bk7 at 457 or 488 nm by using powers below 100 mW did not induce any index changes. We previously observed that bulk Nd-doped Bk7 glass is photosensitive, exhibiting a negative index change of 10^{-4} at 488 nm.[11] Therefore we chose to investigate K^+-ion-exchanged Nd-doped Bk7 glass, which has previously been used as a host for planar waveguide lasers,[13] and hence self-writing offers the possibility of integrating passive and active devices.

The ion-exchanged sample was produced with commercially available Bk7 borosilicate glass doped with 1.5-wt. % Nd_2O_3. The top surface was polished and it was then immersed in molten potassium nitrate at 395 °C for-

1 h to form a 2.5-μm-deep ion-exchanged layer. We observed that this material is photosensitive to both 457- and 488-nm light, with the largest effects obtained at 457 nm. It has an initial refractive index of ~1.5 and the ion-exchanged planar surface layer has an index difference from the bulk material of 0.0092 and 0.0080 at 1 μm for the TM and the TE polarizations, respectively.[13] To our knowledge this is the first report of photosensitivity in K^+-ion-exchanged Nd-doped Bk7. As this glass was also found to exhibit a high degree of spatial homogeneity, we believe it to be ideal for exploration of self-writing and to provide further insights into the photosensitivity mechanisms responsible for the observed index change.

3. EXPERIMENT AND EXPERIMENTAL RESULTS

In these experiments a single-mode cw Gaussian output beam at 457 nm from an argon-ion laser is used as the writing beam. The beam is focused to a waist at the polished input face of the ion-exchanged layer. The light initially diffracts through the material, and the beam that emerges from the layer is monitored over time. If the refractive index increases because of illumination, the output beam should narrow and become more intense as the light becomes guided by the waveguide it induces.

As Fig. 1 indicates, the planar ion-exchanged surface layer in this experiment is thin and relatively long samples were used (6.5 and 14 mm). Hence a careful choice of writing beam width is needed: although a more efficient launch into the layer can be obtained with a narrow beam, the layer cannot confine such a rapidly diffracting beam well, and also a large index increase is required for the self-writing process to overcome the transverse diffraction. Using a circularly symmetrical beam, we found a beam with a full width at half-maximum (FWHM) of 7 μm offers the best compromise. Note that in the future the use of elliptical writing beams would allow the launch into the layer to be optimized independently from the transverse width.

Although self-writing by use of Gaussian writing beams has been conducted in germanosilicate[1] and As_2S_3 chalcogenide[9,10] planar glass, basic self-writing experiments are crucial in any new material to explore the self-writing and photosensitivity processes that occur, and these are presented here for K^+-ion-exchanged Nd-doped Bk7.

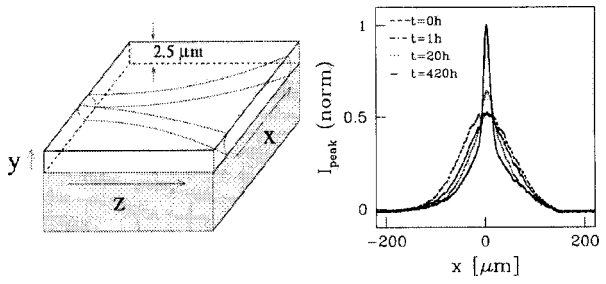

Fig. 1. Left, light propagates in the 2.5-μm-deep ion-exchanged layer. Right, output beam profiles during waveguide evolution (writing wavelength, 457 nm; power, 38 mW; FWHM, 7 μm; sample length, 6.5 mm).

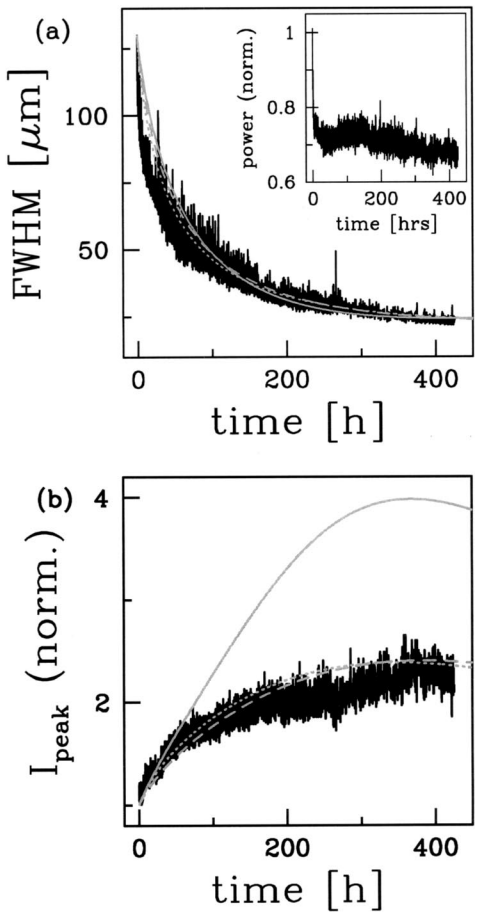

Fig. 2. Change in FWHM and peak intensity at the output face for the experiment shown in Fig. 1 (black) and corresponding simulations (gray). Solid curves ignore loss, dashed curves include L_{PS}, and dotted curves include both L_{PS} and L_C (see text). The inset shows the change in power during the experiment.

In Fig. 1 cross sections of the beam that emerges from the 6.5-mm-long sample are shown during a typical experiment by use of a 38-mW writing beam. The FWHM of the output beam is observed to narrow over time, here in total by a factor of 7, and becomes more intense by a factor of 2.5. Hence the refractive index must increase because of the illumination, which reduces the diffraction of the propagating light that is guided through the evolving waveguide. Note that remarkably good beam quality is obtained, which is a measure of the excellent homogeneity of this glass along the full propagation length.

Figure 2(a) shows the change in FWHM at the output face and how it decreases during this exposure. The corresponding increase in peak intensity is shown in Fig. 2(b). Note how the changes slow down at late times in the experiment as the refractive-index change saturates and no further changes can be induced. Although the output beam continues to evolve throughout the long exposure time, it is worth noting that the initial change in FWHM is extremely rapid.

The total change in power at the output face is shown in the inset in Fig. 2. In this experiment, a decrease by a factor of 1.4 in power is observed, of which 46% is due to a drop in the power of the writing laser early in the experiment. Comparing the propagation loss through an unex-

posed region with that in the SWW reveals an equivalent induced loss during the exposure of 1 dB/cm at the writing wavelength (ignoring the change in coupling into the layer owing to the induced index change).

During all the experiments at 457 nm, a visible red luminescence is generated throughout the sample in positions at which the writing beam is intense. The luminescence is found to be dominated by the emission bands around 900, 1060, and 1350 nm, which is characteristic of Nd-doped silica glasses.[14] Since the spatial distribution of the luminescence reflects the intensity distribution of the propagating beam, it could be a useful tool for monitoring the waveguide evolution. In addition it offers useful information about the glass properties, which could be used to explore the photosensitivity of this material.

All the above-presented results indicate that this glass is photosensitive at 457 nm and show the key evidence that the index increases. We formed a range of channels within this glass that substantially reduce the diffraction of the propagating beam. Finally, in comparison with previous research,[1] an extremely good beam quality is obtained, which indicates that this glass is well suited for self-writing.

4. NUMERICAL MODEL AND SIMULATIONS

To obtain a deeper understanding of the self-writing process and to predict the effects of different experimental parameters, numerical simulations were conducted. This had previously been done for both planar and bulk geometries.[2,3,11]

A. Model for Self-Writing

Here $\Delta n(t, z, x)$ is defined as the refractive-index change that occurs in the planar layer owing to photosensitivity (see Fig. 1). Note that the index difference between the layer and the surrounding regions is assumed to be larger than the index change induced by photosensitivity and thus that Δn is independent of y. Finally, the induced index distribution is initially taken to be uniform throughout the planar layer, i.e., $\Delta n(0, z, x) = 0$.

When the material is illuminated, the locally induced change in refractive index is described by use of a phenomenological model for photosensitivity:

$$\frac{\partial \Delta n(t, z, x)}{\partial T} = I^p(t, z, x)\left[1 - \frac{\Delta n(t, z, x)}{\Delta n_s}\right], \quad (1)$$

where intensity I is EE^* and E is the electric field. A saturation index change, Δn_s, is introduced to limit the change in index that can be induced. This simple phenomenological model has previously been shown to agree well with experiments in planar germanosilicate glass.[1] Note that, if $p = 2$, a two-photon absorption process occurs within the material. T is a normalized time defined as $T = A_p I_0^p t$, where A_p is a real constant that depends on p, the material properties, and the writing wavelength (λ_w), $I_0 = I(t, 0, x)$, and t is the time in seconds.

Here we use the intensity distribution as a Gaussian writing beam with a FWHM of $a\sqrt{2 \ln 2}$. The paraxial approximation is used to describe light propagation as discussed in Refs. 2 and 4. As shown in Section 3 the propagation loss increases during the waveguide evolution, and we assume that the loss per unit length is $L_C + L_{PS}$, where L_C is a constant and uniform loss and $L_{PS}(t, z, x) = \gamma k_0 \Delta n(t, z, x)$ is a photosensitive-induced loss, where γ is a proportionality constant and $k_0 = 2\pi/\lambda_w$. This model for the induced loss has previously been shown to agree with experiments in germanosilicate[2] and chalcogenide glass.[3]

The paraxial wave equation and the photosensitive equation, Eq. (1), along with the writing beam defines the model. When we solve these equations, advantage is taken of the difference in time scales between the light propagation (nanoseconds) and the index evolution (minutes), hence the equations can be solved by use of a split step beam propagation model. When fitting the simulations to experimental data the time in the simulations can be scaled since the normalized time T is used in the model and A_p is unknown. Note that parameter A_p and therefore the normalized time is determined by the details of the material photosensitivity, and hence could be extracted if systematic investigations of a range of experiments were conducted. In most glasses the index change that can be achieved by illumination (typically 10^{-5}–10^{-2}) depends critically on the glass composition. Although the change could be measured experimentally we find that self-writing is a powerful tool to extrapolate the magnitude of change of new materials by choosing Δn_s to fit the experiments.

Once the SWWs are formed, the magnitude of the index change can decay slightly over time. In addition, the induced index change is less at longer wavelengths (λ). These effects can be approximated by

$$\Delta n_{\lambda,t}(\lambda, t, z, x) = D(t)W(\lambda)\Delta n(\lambda_\omega, t_0, z, x) \quad (2)$$

for $t > t_0$, where t_0 is the time when the initial experiment is turned off, $D(t)$ describes the decay in the photosensitive index change, $W(\lambda)$ describes the induced index at longer wavelengths, and Δn is as defined in Eq. (1). Observe from Eq. (2) that we assume that the index in both cases decreases uniformly throughout the sample.

B. Results and Comparison with Experiments

In Fig. 2 results from the numerical simulations (gray lines) are shown together with the experiment. Initially any propagation losses were ignored (solid curves) and excellent agreement for the beam-width evolution was obtained when the saturation refractive index, Δn_s, is 5.2×10^{-5} and $p = 2$. However the change in peak intensity shows a significantly larger increase in the simulations than in the experiments.

It has previously been shown[3,4] that loss has a greater influence on the intensity evolution than on the width. By incorporating a photosensitive-induced loss, L_{PS}, in the model, which induces a larger absorption of light at positions where the index has been altered, the right magnitude of intensity change can be induced (dashed curves in Fig. 2). As in Ref. 2, a constant and uniform loss alone does not improve the agreement with experiments significantly. The dashed curve corresponds to simulations with $\Delta n_s = 5.7 \times 10^{-5}$ and $L_{PS} = 90000 \times \Delta n(z, x)$ dB/cm, i.e., a maximum loss of 5.13 dB/cm is present at positions where Δn_s is reached. However, in

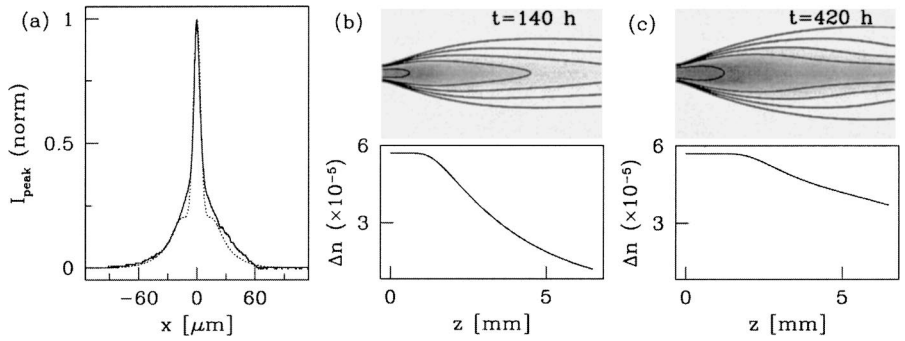

Fig. 3. (a) Final output beam shapes in the 6.5-mm sample: solid curve, experiment and dotted curve, simulation by use of fitted material parameters. (b) and (c) Simulated index distribution during evolution (the contour levels are separated by 2 dB and the transverse distance has been scaled; only the central 0.3-mm region is shown) and cross sections of the index along the propagation axis.

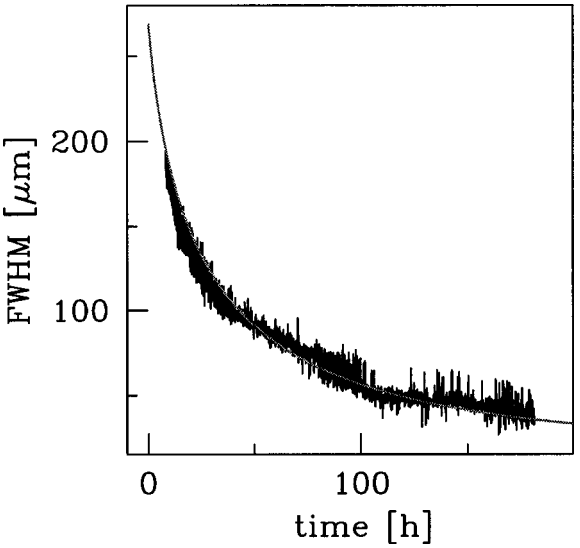

Fig. 4. Experimental and numerical results (by use of fitted material parameters) from the longer (14-mm) sample during the first 175 h. Here power is 20 mW.

reality a constant and uniform propagation loss, L_C, is also present in the material and, by including both types of loss, the agreement could be improved even further for the evolution in both FWHM and peak intensity as shown by the dotted curves in Fig. 2. Here the (fitted) material parameters are $\Delta n_s = 5.7 \times 10^{-5}$, $L_C = 2$ dB/cm, and $L_{PS} = 85000 \times \Delta n(z, x)$ dB/cm, hence a maximum L_{PS} of 4.85 dB/cm occurs at localized positions where Δn_s has been reached. Although these losses appear to be high, the regions of high loss are localized and our experiments indicate that the total loss induced at the writing wavelength is 1 dB/cm.

In Fig. 3(a) the beam that emerges from the shorter sample at the end of the experiment (solid curve) is reproduced from Fig. 1 along with the corresponding simulation by use of the fitted material parameters (dotted curve). The originally Gaussian distribution grows a pedestal in both experiment and simulation during the evolution.

Good agreement is also obtained for experiments carried out in the longer sample by use of the same parameters as above; see Fig. 4 for the first 175-h exposure with a power of 20 mW. The fact that our model also agrees with experiments in this longer sample confirms that this is an excellent model for self-writing and that these material parameters provide a good description of the photosensitivity of K^+-ion-exchanged Nd-doped Bk7.

In the experiments we determined the evolution of the refractive index indirectly by monitoring the propagating writing beam at the output face. However, since Figs. 2–4 show good agreement between experiments and simulations, the numerical simulations can be used as a tool for extracting information about the evolution of the refractive-index distribution within the material. In Figs. 3(b) and 3(c) the index distributions from the simulation are shown for two different times during the evolution, equivalent to 140 and 420 h in the experiment in the shorter (6.5-mm-long) sample shown in Fig. 2. The cross sections along the propagation axis show that the index initially grows more quickly near the input face where the light intensity is highest and how, over time, it penetrates further along the propagation axis into the material.

The above results prove K^+-ion-exchanged Nd-doped Bk7 to be photosensitive to light at 457 nm and that waveguides can be self-written in this glass. As the sample is homogeneous throughout the layer it is straightforward to locate the channel after the exposure and also to reproduce the experiments. In addition, since different samples have been used it has proved to be a reliable and consistent material. Consequently it promises to be an excellent host for self-writing, offering the possibility of extending and developing the process further. The fact that the numerical simulations describe the different experiments extremely well by use of physically reasonable values for the material parameters validates the simple phenomenological model used. Finally, this excellent agreement can be used to characterize the photosensitivity that occurs during self-writing as described in the following section.

5. INVESTIGATION OF PHOTOSENSITIVITY

A. Decay of Index Change

To investigate whether the induced photosensitive index changes are permanent, we sent a beam through the waveguide after the initial exposure. One can observe any decay in index by monitoring the increase in the FWHM over time. Figure 5(a) shows that a small decay

in index is present over a time scale of several weeks. Note that the sample was not annealed, a technique that is often used to fix the index change.

This technique monitors the change in index indirectly. To extract the magnitude of this decay the simulations can be used to determine the relationship between index change and output beam width. This is done by application of a spatially uniform decay by a factor of $D(t)$ as in Eq. (2) to the index distribution created in our simulations. By propagating light through this modified index distribution, we can link the index decay to the FWHM of the output beam, as shown by the inset in Fig. 5(a), where $\Delta n_{\lambda,t}(\lambda, t, 0, 0)$ is the largest index change present in the structure (which is in general Δn_s). Even when the index change has decayed to half of its original value, here 2.85×10^{-5}, the beam width has only increased by 15%.

In Fig. 5(b) the widths from the reexposures shown in Fig. 5(a) have been converted into index change by use of the above mapping, which shows that on a time scale of months an index change of 4.25×10^{-5}, i.e., 75%, is still present. Note that the time in this graph is measured from the point at which the initial experiment was turned off. The decay in refractive index can be described by use of a model previously applied to investigate the relaxation of photosensitive index changes in UV-induced fiber Bragg gratings[15]: $\Delta n_{\lambda,t}(\lambda, t, 0, 0) = 1 - at^b + c$, where a, b, and c are constants chosen to fit the experimental data. This numerical fit is shown as a solid curve in Fig. 5(b), where $a = 1.04 \times 10^{-6}$, $b = 0.24$, and $c = -0.999942$. To predict the long-term aging effects, this model was used to extrapolate the decay in the induced refractive index [see inset in Fig. 5(b)]. Even after a decade nearly half of the index change still remains, which shows that the waveguide would still reduce the diffraction of a propagating beam by a factor of nearly 3.5 relative to free diffraction.

B. Dependence on Writing Power

Photosensitive index changes are known to occur more rapidly as the power increases although it is difficult to monitor the change directly. Self-writing can be used as a tool to investigate the relationship between power and speed of index change and here the early stages of waveguide evolution are studied, where the index change has not yet saturated. In addition, in these early times the greatest increase in index is induced at the input face,

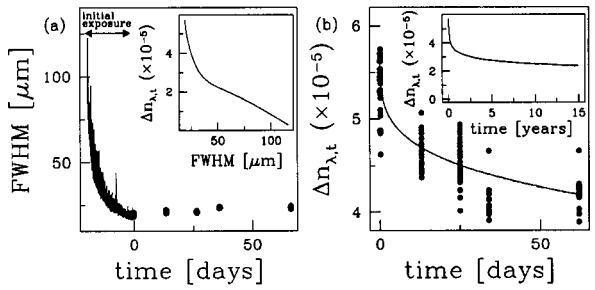

Fig. 5. (a) Initial experiment together with reexposures. The inset shows the relationship between output FWHM and Δn. (b) Corresponding decay in index after the initial exposure and a numerical fit. The inset shows the index decay prediction over a time scale of years.

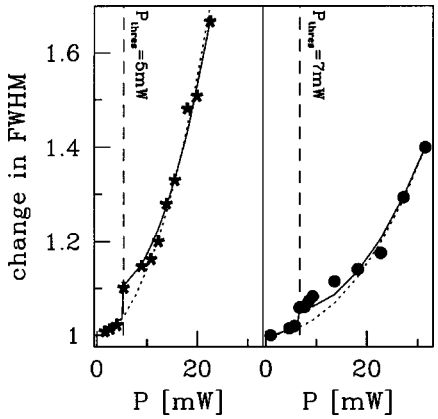

Fig. 6. Factor by which the FWHM is reduced during the first hour of exposure at different input powers. Stars, experiment with a 7-μm beam; dots, 12.5-μm beam. Dotted curves, corresponding simulation by use of the original numerical model; solid curves, the model including an intensity threshold. Note that all the simulations assume that $p = 2$, $\Delta n_s = 5.2 \times 10^{-5}$, and no loss.

which acts as a focusing lens, and the reduced diffraction of the propagating writing beam reflects the strength of this lens.

Here the factor by which the FWHM is reduced during a 1-h experiment at the output face of the sample is determined by use of different writing powers (for a fixed writing beam width). Results for a 7-μm beam in a 14-mm-long sample are represented by stars in Fig. 6. Note that the change in width reflects the magnitude of induced refractive-index increase. It is evident that the process proceeds faster at higher powers. This is consistent with the numerical model for the photosensitivity described by Eq. (1), where the index change depends on the intensity squared for this two-photon absorption process, and corresponding numerical simulations (dotted curve) verify this. In addition the experimental results reveal a threshold in writing power at approximately 5 mW: no index changes are induced at lower powers. The smoothness of this experimentally obtained curve reflects the excellent homogeneity of our sample (since each data point corresponds to a different part of the sample).

To gain a more complete understanding of these results, the same experiments were also performed for a wider beam with a FWHM of 12.5 μm. This is indicated by dots in Fig. 6, and corresponding simulation results are shown by the dotted curve. A threshold in power is again observed, this time at a higher power of 7 mW. Comparison of the two sets of experiments shows a steeper curve (and therefore faster process) for the narrower beam. This is not surprising because the narrower beam has a higher peak intensity at the same writing power. Note that the peak intensities that correspond to the power threshold differ for the two beam sizes.

As described above, good agreement between experiments and simulations was obtained for both beam sizes when higher powers were used, however this numerical model for the index change cannot reproduce the observed threshold behavior. Indeed, the simple model in Section 4 always induces the same final index distribution regardless of the peak intensity (although longer times are

needed for lower intensities), and so a new model is required to describe the threshold. This new model must significantly modify the index change near the threshold so as to enhance the change just above the threshold and reduce it sharply below. It must also exhibit the same behavior at high intensities as the simple model. This can be achieved by modification of Eq. (1) in the following manner:

$$\frac{\partial \Delta n}{\partial T} = \left| I^2 + \alpha I \tanh\left(\frac{\beta}{I - I_{\text{thres}}}\right)\right| \left(1 - \frac{\Delta n}{\Delta n_s}\right), \quad (3)$$

where α and β are chosen to fit the experimental data and I_{thres} is an intensity threshold derived from the measured power threshold. When we compared the results using this model with the experiments an excellent agreement for the speed of the process was obtained for both widths, solid curves in Fig. 6, where $\alpha = 600$ and $\beta = 0.002$.

Although it is likely that a similar threshold behavior could be induced by use of other models, we found this to be the simplest model that resulted in good agreement with experiments. In addition, this modified model gives similarly good agreement as the original model for the total waveguide evolution (not shown here for brevity). Note that, when operating close to the material threshold, separate simulations are needed for different writing powers. However, at high powers the simpler original model gives good results, hence the threshold can be ignored. The accurate prediction of the observations for all the data suggests that the model describes the material well and is likely to be a useful tool for investigating photosensitivity not only for the development of SWWs, but also for writing gratings or other photolithography applications such as direct-writing techniques.

6. GUIDING LIGHT IN THE SELF-WRITTEN WAVEGUIDE

A. Experimental Observations

To investigate the guidance properties of the waveguides self-written in our experiments, Gaussian beams of different sizes and light at longer wavelengths were launched into the structure. During the initial experiment we used a writing beam with a FWHM of 7 μm at 457 nm, and the resulting SWW reduced the diffraction of light by a factor of 7. Here beams with a FWHM ranging between 2.5 and 7 μm are launched into the waveguide. We quantified the effect of the SWW on the launched beams by measuring the reduced diffraction, which is defined to be the ratio between the width of a beam that emerges from an unexposed region to that emerging from the waveguide. In Fig. 7(a) the dots show the result of this investigation at 457 nm. This reveals a more dramatic light confinement for narrower beams, which is due to the fact that narrow beams exhibit a larger free diffraction than that of wider beams, hence a greater reduction in diffraction is possible. However, for the narrowest beams, the waveguide is not strong enough to confine this rapidly diffracting beam entirely. We obtained a good example of a narrow but still well-confined beam by using a beam with a FWHM of 3 μm; see Fig. 8(a), where a cross section of the beam that emerges from the waveguide is shown as a dashed curve. It is clear that the light is well confined in the channel when the data are compared with the equivalent beam that diffracts in a uniform material (solid curve). Note that these experiments were carried out at powers well below threshold, hence no further index changes were induced during characterization.

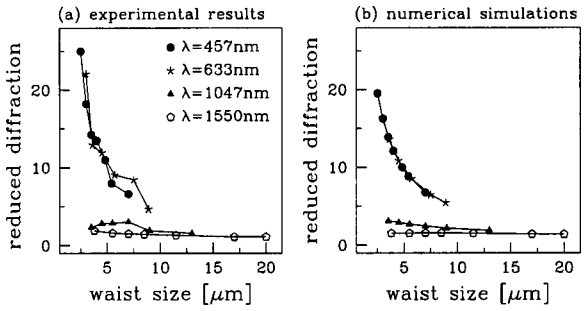

Fig. 7. Reduced diffraction in a SWW in comparison with a uniform material for a range of beam sizes.

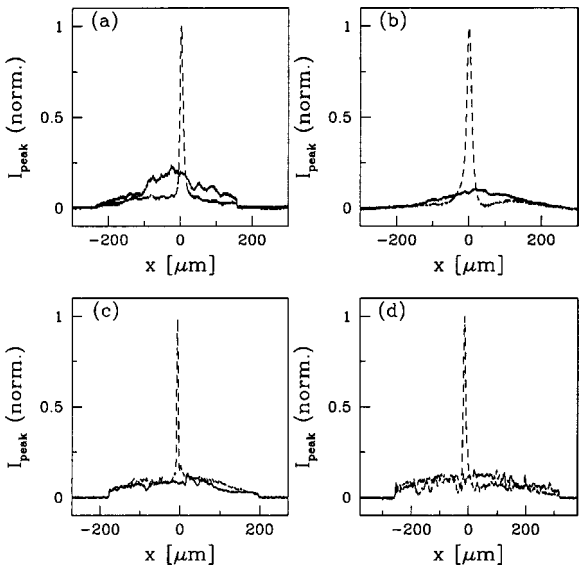

Fig. 8. Dashed curves, beams that emerge from the waveguide; solid curves, propagation in a uniform material. (a) Front launch at 457 nm by use of an input FWHM of 3 μm, (b) front launch at 633 nm by use of a FWHM of 3.6 μm, (c) back launch into the waveguide at 457 nm, (d) back launch at 633 nm.

These SWWs will ultimately be most useful at longer wavelengths where the index change will be somewhat lower than at the writing wavelength (457 nm). Here light at longer wavelengths is launched into the SWW to determine the guidance properties and also to extract the index change at these wavelengths. In Fig. 8(b) we can see that good confinement of light is also obtained at 633 nm, here for a beam with a FWHM of 3.6 μm. The summary in Fig. 7(a) shows that similar guidance was obtained at 457 and 633 nm. At 1047 and 1550 nm a somewhat weaker guidance was found, although a significant reduction by a factor of 3 is still present at 1047 nm, which shows that these waveguides guide light over a broad wavelength band. In addition, the photoinduced loss through the channel is significantly smaller at the longer wavelengths; at 633 nm the induced loss is 0.5 dB/cm and at 1047 nm it is 0.25 dB/cm, in comparison with 1 dB/cm at the writing wavelength (the difference in

coupling to the waveguide at different wavelengths has been ignored).

Finally the sample was turned around and light launched in from the back of the SWW. This resulted in a strong confinement of the central part of the beam; see Figs. 8(c) and 8(d) for 457 and 633 nm. Observe that some of the light remains in a low-level pedestal. The reason not all the light gets trapped because the SWW is not uniform, i.e., the index difference at the end is not as large as at the beginning; see Fig. 3(b) where the index distribution is shown. Hence, since the propagating light diffracts rapidly close to the input face, where the index difference is now relatively small, less light is confined to the waveguide. However, still 25% of the power at the output face is trapped in the center peak and at both 457 and 633 nm. By using input beam widths of 4 (at 457 nm) and 3.6 μm (at 633 nm), we obtained an enormous reduced diffraction by a factor of 40, largely because of the high-index change near the original input face that acts as a lens. This results in a more uniform waveguide for the light that does get trapped: we observed the propagating light to grow in width by just a factor of 1.2 from input to output at 457 nm and by a factor of 2 at 633 nm, compared with 5 and 7 when front launching.

B. Comparison with Numerical Simulations

To compare the results in Subsection 6.A with simulations, light is allowed to propagate through the index distribution calculated from the full simulations presented in Section 4. Figure 7(b) shows the numerical results that correspond to the experiments shown in Fig. 7(a). At 457 nm (dots) and at 633 nm (stars) we obtained excellent agreement between experiment and simulations, which shows that no degradation of the index change is present at 633 nm. In addition, this is a powerful test of the numerical model used, which confirms that the simulations do indeed create a refractive-index distribution similar to that formed in the experiment and that the numerically induced spatial distribution in the index change is accurate, since differently sized beams propagate in the same way as observed experimentally. Note also that no free parameters exist in these simulations. In addition this shows that the model that describes the time evolution in this cumulative process is valid.

As already mentioned, at longer wavelengths the effective index change is typically smaller than at the writing wavelength, and this can also be quantified by use of the numerical simulations. At 1047 and 1550 nm the magnitude of index change is decreased according to Eq. (2) in Section 4. If the index change is reduced to 45% of its original value, i.e., $W(\lambda) = 0.45$ hence $\Delta n_s = 2.6 \times 10^{-5}$, good agreement with experiments at 1047 nm can be obtained; see triangles in Fig. 7. The equivalent result for light at 1550 nm is represented by circles, and here the index needs to be reduced to 40% of the original change, i.e., $\Delta n_s = 2.3 \times 10^{-5}$, to fit the experiments. The good agreement with experiments indicates that the guidance at all wavelengths within the SWW can be described by making this straightforward modification to the numerical model.

Numerical simulations have also been carried out corresponding to the experiments when launching light from the back of the sample. Here a qualitative agreement is obtained. We believe that possible differences in the induced index distributions formed in the simulations to that in the experiment accumulate further into the material and the largest discrepancies will be found at the output face. Also small imperfections in the glass are more noticeable when the index change is smaller, i.e., close to the output face. Hence, although these errors are negligible when light is sent in from the front, they have a more significant effect when light is launched from behind.

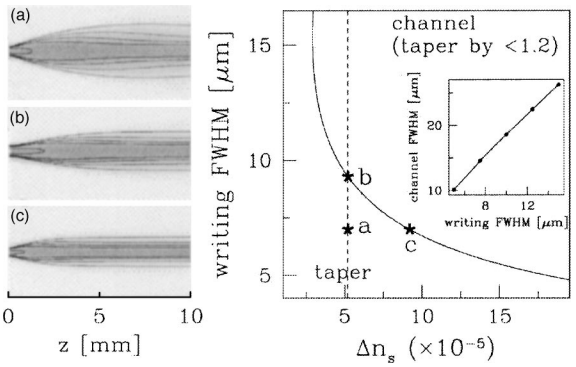

Fig. 9. Left, index distribution for (a) FWHM = 7 μm, $\Delta n_s = 5.2 \times 10^{-5}$ as in our experiment; (b) FWHM of 9 μm, $\Delta n_s = 5.2 \times 10^{-5}$; (c) FWHM of 7 μm, $\Delta n_s = 9 \times 10^{-5}$. Right, waveguide shape as a function of FWHM and Δn_s: above the curve, channels are formed and below, tapers are obtained. The inset shows the relationship between the FWHM and the resulting channel width.

7. OPTIMIZING THE SELF-WRITING PROCESS

For a given beam, the structure that evolves is determined by the achievable index change in the material. By use of a Gaussian beam, channels form if the material exhibits a large enough increase to overcome diffraction totally, otherwise the evolution stops earlier and a taper forms. Here we use our experimentally validated simulations to predict whether tapers or channels form for a range of experimental conditions. This is done for a 1-cm-long sample, and losses in the material are ignored for simplicity.

The structure that results by use of our experimental parameters (FWHM of 7 μm, writing wavelength of 457 nm) can be seen as (a) at left in Fig. 9. This structure tapers in width by a factor of 1.7 in the 1-cm-long sample. To investigate ways of making more uniform channels, we perform simulations to explore the SWWs that form for a range of different values of the writing FWHM and saturation index change. Using these simulations, we identify the conditions under which a relatively uniform channel waveguide forms. Here we define a channel as a refractive-index distribution that tapers in width by less than a factor of 1.2 from input to output. By use of this definition, experiments located above the curve in the right part of Fig. 9 result in channels, whereas below the curve tapers are formed. Note that the relationship between the writing FWHM and the width of the resulting channel is nearly linear; see the inset at right in Fig. 9.

At right in Fig. 9 it can be seen that, although our experiment (a) produced a tapered waveguide, a channel can form in this material by use of a wider beam, for example, 9 μm, as in (b). Using a material with a slightly larger index change of 9×10^{-5}, narrower channels can be created as shown by (c). From this it is evident that, to form narrow channels, a material with a large index change is required, which is due to the fact that narrow beams diffract more rapidly than wider beams and hence a larger change is needed to counteract this diffraction. It can be seen in the graph that the possible self-written channel widths are in a range that is suitable for integration with fibers and other devices and that relatively small index changes are needed to write these waveguides. The photosensitivity of the material used here has not been optimized, and we believe that, by exploring different Nd-doped concentrations and ion-exchange conditions, the index change could be increased.

8. DISCUSSION AND CONCLUSION

We have investigated the photosensitivity process in K^+-ion-exchanged Nd-doped Bk7. This material exhibits a refractive-index increase of 5.7×10^{-5} under illumination at 457 nm by use of powers up to 40 mW. In comparison with most previous self-writing experiments reported in glass, our material is found to exhibit the excellent homogeneity required to reproduce the experiments successfully and to compare results by use of different experimental parameters. This has allowed information to be extracted about the photosensitivity process that occurs within the material. This material exhibits a power threshold in photosensitivity that depends on the beam size. By use of a writing beam of 7 μm, no index changes are induced below 5 mW, and, for a wider beam of 12.5 μm, the threshold is 7 mW. The physical mechanism that causes this threshold is at present unclear. Investigation of the sample input face with a microscope reveals that no obvious physical damage occurs during exposure. It is possible that the threshold could exist because a finite energy is required to cause structural rearrangements and thus change the refractive index. In practice, this threshold is useful when characterizing the waveguide after exposure, since low-power illumination does not induce additional changes. This is particularly important in a material such as the one used here for which the early index changes occur rapidly.

The self-writing process proceeds faster at higher peak intensities, hence use of a higher writing power increases the writing speed, although of course a dramatic increase would ultimately damage the sample. Another way to increase the peak intensity would be by use of a narrower writing beam. As long as a sufficient index change is possible in the sample, narrower waveguides could be written at higher speeds.

Investigation of the aging of the induced index changes have been carried out. This revealed that the index changes are long lasting and that half of the change will remain for at least a decade. In addition the waveguides can be used to guide light at longer wavelengths: they guide well at 633 nm, although the guidance at 1047 and 1550 nm is somewhat weaker. The guidance at these longer wavelengths could be improved if slightly larger index changes were induced, which would be possible by optimization of the photosensitivity within the material.

We have also shown that numerical simulations of the process provide a good description of the experiments. When modeling experiments that are carried out close to the power threshold a modification to the model that incorporates this property is needed. Here a suitable model has been developed that provides good agreement with experiments.

Note that in all the simulations carried out the index changes are assumed to affect only the beam in the transverse direction. Although the excellent agreement with experiments show that this assumption is reasonable, it could be possible to improve our numerical description in the future by carrying out bulk simulations. In this way, we could take into account the alterations in launch conditions into the layer during the evolution. In addition, we have previously found that bulk Nd-doped Bk7, used as host to the planar ion-exchanged layer, exhibits a decrease in index when exposed to blue light.[3] Since some of the propagating light illuminates the bulk of the material during the self-writing process, this would also affect the launch conditions as the index difference between layer and bulk therefore increases during illumination.

Because of the excellent agreement between experiment and simulations throughout this paper, we used the numerical simulations to investigate how the choice of different experimental parameters influences the final waveguide structure. This shows that, when a Gaussian writing beam is used in a material with a specific possible index change, the resulting structure depends critically on the writing beam size, which determines whether a channel or taper forms in response to illumination.

Our observations indicate that K^+-ion-exchanged Nd-doped Bk7 is an ideal host for self-writing experiments. Here we have developed a reliable numerical model that provides a good description of self-writing in this material and, when used in conjunction with experiments, can be used to characterize the photosensitivity of the material. Hence we anticipate that this material should provide a platform for further development of the self-writing process in glass. Since the photosensitivity of this material has not been optimized, it is likely that larger index changes should be possible. Ultimately, self-writing should allow the formation of waveguide structures that can be directly integrated with existing devices. In addition, it offers the prospect of forming complex, low-loss, waveguide structures without translating either the sample or the writing beam.

ACKNOWLEDGMENTS

We thank Dave Shepherd and Simon Hettrick, Optoelectronics Research Centre, University of Southampton, for their help in fabricating the glass samples and also for helpful discussions. Tanya Monro acknowledges the support of a Royal Society University Research Fellowship.

The e-mail address for A. Ljungstrom is aml @orc.soton.ac.uk.

REFERENCES

1. T. M. Monro, D. Moss, M. Bazylenko, C. M. de Sterke, and L. Poladian, "Observation of self-trapping of light in a self-written channel in photosensitive glass," Phys. Rev. Lett. **80**, 4072–4075 (1999).
2. T. M. Monro, C. M. de Sterke, and L. Poladian, "Investigation of waveguide growth in photosensitive germanosilicate glass," J. Opt. Soc. Am. B **13**, 2824–2832 (1996).
3. A. M. Ljungström and T. M. Monro, "Light-induced self-writing effects in bulk chalcogenide glass," J. Lightwave Technol. **20**, 78–85 (2001).
4. T. M. Monro, C. M. de Sterke, and L. Poladian, "Analysis of self-written waveguide experiments," J. Opt. Soc. Am. B **16**, 1680–1685 (1999).
5. S. Shoji, S. Kawata, A. A. Sukhorukov, and Y. S. Kivshar, "Self-written waveguides in photopolymerizable resins," Opt. Lett. **27**, 185–187 (2002).
6. S. S. Sarkisov, V. Grimalsky, M. J. Curley, G. Adamovsky, and C. Martin, "Connection of two-dimensional optic fiber arrays using optical beam self-trapping in photocurable media," in *Micro- and Nano-Optics for Optical Interconnection and Information Processing*, M. R. Taghizadeh, H. Thienport, and G. E. Jabbour, eds., Proc. SPIE **4455**, 107–118 (2001).
7. N. Hirose and O. Ibaragi, "Optical solder effects of self-written waveguides in optical circuit devices coupling," in *Electronic Components Technology Conference* (Institute of Electrical and Electronics Engineers, Piscataway, N.J., 2002).
8. W. S. Brocklesby, S. J. Field, D. C. Hanna, A. C. Large, J. R. Lincoln, D. P. Shepherd, and A. C. Tropper, "Optically written waveguides in ion implanted $Bi_4Ge_3O_{12}$," Opt. Mater. **1**, 177–184 (1992).
9. C. Meneghini and A. Villeneuve, "As_2S_3 photosensitivity by two-photon absorption: holographic gratings and self-written channel waveguides," J. Opt. Soc. Am. B **15**, 2946–2950 (1998).
10. N. Hô, J. M. Laniel, R. Vallée, and A. Villeneuve, "Creation of microchannels in a photosensitive As_2S_3 slab waveguide," J. Opt. Soc. Am. B **19**, 875–880 (2002).
11. A. M. Ljungström and T. M. Monro, "Observation of light-induced refractive index reduction in bulk glass and application to the formation of complex waveguides," Opt. Express **10**, 230–235 (2002), http://www.opticsexpress.org.
12. J. E. Roman and K. A. Winick, "Photowritten gratings in ion-exchanged glass waveguides," Opt. Lett. **18**, 808–810 (1993).
13. S. J. Hettrick, J. I. Mackenzie, R. D. Harris, J. S. Wilkinson, D. P. Shepherd, and A. C. Tropper, "Ion-exchanged tapered-waveguide laser in neodymium-doped BK7 glass," Opt. Lett. **25**, 1433–1435 (2000).
14. S. B. Poole, D. N. Payne, R. J. Mears, M. E. Fermann, and R. I. Laming, "Fabrication and characterization of low-loss optical fibers containing rare-earth ions," J. Lightwave Technol. **LT-4**, 870–875 (1986).
15. T. Erdogan, V. Mizrahi, P. J. Lemaire, and D. Monroe, "Decay of ultraviolet-induced fiber Bragg gratings," J. Appl. Phys. **76**, 73–80 (1994).